General Buckling of Cylindrical Reticulated Shell Roofs

Tsutomu KOKAWA

Graduate Student of Tokyo Metropolitan University, Tokyo

The general buckling behaviors of Cylindrical Reticulated Shell Roofs (C.R.S.R.) are considerably influenced by the reticular pattern, shell geometry, boundary condition and load distribution. To grasp the general buckling behaviors of C.R.S.R. under these items, a method of approximate analysis is developed by treating them as continuum structures. Based on this method, the general buckling behaviors of isotropic C.R.S.R. are investigated numerically under various shell geometries, generator boundaries, symmetrical or unsymmetrical normal load with respect to the central generator, in comparison with the classical buckling load of the closed cylinder subjected to a uniformly normal load.

I. INTRODUCTION

Single layer reticulated shells made of lightweight shapes or pipes are easily applicable in construction. On the other hand, they have a defect against the general instability because of low bending rigidity. Therefore, it is important to confirm safety against general buckling[1,2]. However, there is scarcely any information for the general buckling of both reticulated and monocoque cylindrical shell roofs in contrast to the large number of fruitful results for the closed cylinder[3,4]. The general buckling behaviors of Cylindrical Reticulated Shell Roofs (C.R.S.R.) formed from an assembly of triangular grids composed of longitudinal and diagonal members are considerably influenced by the mechanical properties of a reticular element, shell geometry, boundary condition and load distribution.

The purpose of this study is to make clear theoretically the general buckling behaviors C.R.S.R. based on continuous treatment, paying attention to the above four items. As a link in the chain of study, this paper contains the following.

(1) An approximate analytical method of deriving the geometrically nonlinear basic equations which govern the general buckling phenomena of C.R.S.R. subjected to normal load is developed under the boundary conditions that the two ends of the structure are simply supported and the two generator edges are arbitrary.

(2) Based upon this method, the general buckling behaviors of isotropic C.R.S.R. are investigated numerically under various shell geometries, generator boundary conditions, symmetrical or unsymmetrical load with respect to the central generator, in comparison with the classical buckling load of the closed cylinder.

II. NONLINEAR BASIC EQUATIONS

1) Basic Equations

Nonlinear basic equations of C.R.S.R. shown in Fig. 1, are given by the following equations:[5]

Compatibility Equation:

$$F^{\cdots} + \left(\frac{\gamma}{\sin^2\alpha\cos^2\alpha}\, 2\, \cot^2\alpha\right)\beta^2 F''^{\cdot\cdot} + \left(\cot^4\alpha + \frac{\gamma}{\sin^4\alpha}\right)\beta^4 F'''' = -\mu_h\beta^2 W'' + \beta^2\,(W'^{\cdot 2} - W''W^{\cdot\cdot}) \tag{1a}$$

Equilibrium Equation:

$$\frac{3}{32}\left\{W^{\cdot\cdot\cdot\cdot} + 6\,\cot^2\alpha\beta^2 W''^{\cdot\cdot} + \left(\cot^4\alpha + \frac{\zeta}{\sin^4\alpha}\right)\beta^4 W''''\right\} = \mu_h\beta^2 F'' + \Lambda(Y) + \beta^2(F^{\cdot\cdot}W'' + F''W^{\cdot\cdot} - 2F'^{\cdot}W'^{\cdot}) \tag{1b}$$

Where $W = \frac{w}{t_h}$, $F = \frac{\varphi}{E_h t_h{}^3}$, φ: stress function, $\mu_h = \frac{B^2}{Rt_h}$, $B = R\theta_0$, $\beta = \frac{B}{L}$, $t_h = \sqrt{\frac{32}{3\gamma}}\; i \sin^2\alpha$, i:radius of inertia of diagonal member, $E_h = \frac{\sqrt{3}}{2\sqrt{2}}\sqrt{\gamma}\,\gamma\frac{\bar{A}}{i\sin^2\alpha}E$, $\gamma = \frac{\bar{A}_x}{2\bar{A}}$, $\zeta = \frac{\bar{I}_x}{2\bar{I}}$, $(\bar{A},\bar{A}_x)$, $(\bar{I},\bar{I}_x)$: average sectional area, moment of inertia per unit width of diagonal, longitudinal member, E: Young's modulus of members, $\Lambda(Y) = \Lambda_s + \Lambda_a G(Y)$, $\Lambda_s = \frac{q_s}{E_h}\left(\frac{B}{t_h}\right)^4$ $\Lambda_a = \frac{q_a}{E_h}\left(\frac{B}{t_h}\right)^4$, $G(Y) = \begin{cases} 1 & Y \geqq 0 \\ -1 & Y \leqq 0 \end{cases}$ $X = \frac{x}{L}$, $' = \frac{\partial}{\partial X}$, $Y = \frac{y}{B}$, $\cdot = \frac{\partial}{\partial Y}$

Member forces and deflections in X, Y direction are represented by using W, F.

$$\left.\begin{aligned} N_2^1 &= \frac{E_h t_h{}^3}{2B^2}\left(\frac{\beta^2}{\sin^2\alpha}F'' \mp \frac{\beta}{\cos\alpha\sin\alpha}F'^{\cdot}\right),\ N_x = \frac{E_h t_h{}^3}{B^2}(-\cot^2\alpha\beta^2 F'' + F^{\cdot\cdot}) \\ M_2^1 &= -\frac{3E_h t_h{}^4}{64B^2\sin^4\alpha}(\beta^2\cos^2\alpha W'' \pm \beta\sin 2\alpha W'^{\cdot} + \sin^2\alpha\, W^{\cdot\cdot}) \\ M_x &= -\frac{3E_h t_h{}^4}{32B^2\sin^4\alpha}\beta^2 W'',\ U' = \frac{t_h{}^2}{B^2}\left(F^{\cdot\cdot} - \cot^2\alpha\beta^2 F'' - \frac{1}{2}\beta^2 W'^2\right), \\ V^{\cdot} &= \frac{t_h{}^2}{B^2}\left\{\left(\cot^4\alpha + \frac{\gamma}{\sin^4\alpha}\right)\beta^2 F'' - \cot^2\alpha F^{\cdot\cdot} + \mu_h W - \frac{1}{2}W^{\cdot 2}\right\} \\ U^{\cdot} + \beta^2 V' &= -\frac{t_h{}^2}{B^2}\beta^2\left(\frac{\gamma}{\sin^2\alpha\cos^2\alpha}F'^{\cdot} + W'W^{\cdot}\right) \end{aligned}\right\} \tag{2}$$

where N, M denote average axial force, bending moment per unit width of member, respectively and $U = \frac{u}{L}$, $V = \frac{v}{B}$.

2) Boundary Equations

Equations of boundary condition are derived by considering member forces acting along the edge together with Eqs. (2). When the two ends are simply supported, considering

$$W = (M_1 + M_2)\,\cos^2\alpha + M_x = (N_1 + N_2)\,\cos^2\alpha + N_x = V = 0;\ X = 0,1$$

and Eqs. (2), the boundary equations become

$$W = W'' = F'' = F^{\cdot\cdot} = 0 \; ; \; X = 0, 1 \tag{3}$$

The following three boundary conditions along the generator edges ($Y = \pm 0.5$) are considered in this paper:

(a) Pinned edge: from

$$W = (M_1 + M_2) \sin^2\alpha = U = V = 0$$

and Eqs. (2),

$$W = W^{\cdot\cdot} = F^{\cdot\cdot} - \cot^2\alpha\beta^2 F'' = \int_0^{\pm 1/2} \left\{ \left(\cot^4\alpha + \frac{\gamma}{\sin^4\alpha} \right) \beta^2 F'' - \cot^2\alpha F^{\cdot\cdot} + \mu_h W - \frac{1}{2} W^{\cdot 2} \right\}$$

$$dY - \int_0^X \left[\left(\int_{1/2}^t \frac{1}{\beta^2} \left\{ F^{\cdot\cdot\cdot} - \cot^2\alpha\beta^2 F''^{\cdot} - \frac{1}{2}\beta^2 (W'^2)^{\cdot} \right\} \Big|_{Y=0} dX + \frac{\gamma}{\sin^2\alpha\cos^2\alpha} F'^{\cdot} \mid_{Y=0} + W' W^{\cdot} \right.$$

$$\left. \mid_{Y=0} \right) \Big] dt = 0 \tag{4a}$$

where the fourth equation of Eqs. (4a) is obtained by considering the symmetry with respect to the central arc.

(b) Simply supported edge: from

$$W = (M_1 + M_2) \sin^2\alpha = (N_1 + N_2) \sin^2\alpha = U = 0$$

and Eqs. (2),

$$W = W^{\cdot\cdot} = F'' = F^{\cdot\cdot} = 0. \tag{4b}$$

(c) Free edge: from

$$(M_1 + M_2) \sin^2\alpha = 2. \frac{\partial (M_1 - M_2)}{\partial x} \sin\alpha\cos\alpha + \frac{\partial (M_1 + M_2)}{\partial y} \sin^2\alpha = N_1 = N_2 = 0$$

and Eqs. (2),

$$W^{\cdot\cdot} + \cot^2\alpha\beta^2 W'' = W^{\cdot\cdot\cdot\cdot} + 5\cot^2\alpha\beta^2 W^{\cdot\cdot} = F'' = F'^{\cdot} = 0. \tag{4c}$$

III. APPROXIMATE ANALYTICAL METHOD

Under the boundary conditions that the two ends of the structure are simply supported (Eq.(3)) and the two generator edges are arbitrary (for example, Eqs.(4)), the nonlinear basic equations(1) are solved by the approximate analytical method given below.

1) Nonlinear Simultaneous Ordinary Differential Equations

Considering Eq. (3), W, F can be given by the following series:

$$\left.\begin{aligned} W &= \sum_m f_m \sin m\pi X = \sum_m (f_{ms} + f_{ma}) \sin m\pi X \\ F &= \sum_m g_m \sin m\pi X = \sum_m (g_{ms} + g_{ma}) \sin m\pi X \end{aligned}\right\} \tag{5}$$

where f_m, g_m are a function of Y only. From the symmetry with respect to the central arc, $m = 1,3,5, \cdots$. Subscripts s, a indicate symmetry and antisymmetry with respect to the central generator, respectively. Substitution of Eqs. (5) into Eqs. (1) and applying Kantrovich's method over the interval (0.,1.) for X, then separating the symmetrical and antisymmetrical parts with respect to the central generator, the following equations are obtained:

a) Symmetrical part:

compatibility eq.;

$$\begin{aligned} \Delta_{1m} g_{ms} = \mu_h \beta^2 m^2 \pi^2 f_{ms} + 2\beta^2\pi^2 \sum_i \sum_j \{ij(f_{is}' f_{js}' + f_{ia}' f_{ja}') p_{ijm} \\ + i^2 (f_{is} f_{js}'' + f_{ia} f_{ja}'') q_{ijm}\} = \Phi_{ms}(Y) \end{aligned} \tag{6a}$$

equilibrium eq.;

$$\begin{aligned} \Delta_{2m} f_{ms} = -\mu_h \beta^2 m^2 \pi^2 g_{ms} + \frac{4}{m\pi} \Lambda_s - 2\beta^2\pi^2 \sum_i \sum_j [\{i^2 (f_{is} g_{js}'' + f_{ia} g_{ja}'') + j^2 (f_{is}'' g_{js} \\ + f_{ia}'' g_{ja})\} q_{ijm} + 2ij (f_{is}' g_{js}' + f_{ia}' g_{ja}') p_{ijm}] = \Psi_{ms}(Y) \end{aligned} \tag{6b}$$

b) Antisymmetrical part:

compatibility eq.;

$$\begin{aligned} \Delta_{1m} g_{ma} = \mu_h \beta^2 m^2 \pi^2 f_{ma} + 2\beta^2\pi^2 \sum_i \sum_j \{2ij f_{is}' f_{ja}' p_{ijm} + (i^2 f_{is} f_{ja}'' \\ + j^2 f_{is}'' f_{ja}) q_{ijm}\} = \Phi_{ma}(Y) \end{aligned} \tag{6c}$$

equilibrium eq.;

$$\begin{aligned} \Delta_{2m} f_{ma} = -\mu_h \beta^2 m^2 \pi^2 g_{ma} + \frac{4}{m\pi} \Lambda_a G(Y) - 2\beta^2\pi^2 \sum_i \sum_j [\{i^2 (f_{is} g_{ja}'' + f_{ia} g_{js}'') + j^2 (f_{is}'' g_{ja} \\ + f_{ia}'' g_{js})\} q_{ijm} + 2ij (f_{is}' g_{ja}' + f_{ia}' g_{js}') p_{ijm}] = \Psi_{ma}(Y) \end{aligned} \tag{6d}$$

where $m, i, j = 1,3,5, \ldots$, $\Delta_{1m} = \cdots\cdots - \beta^2 m^2 \pi^2 \left(\frac{\gamma}{\sin^2\alpha \cos^2\alpha} - 2 \cot^2\alpha \right)'' + \beta^4 m^4 \pi^4 \left(\cot^4\alpha + \frac{\gamma}{\sin^4\alpha} \right)$, $\Delta_{2m} = \frac{3}{32} \{\cdots\cdots - 6 \cot^2\alpha \beta^2 m^2 \pi^2 \cdot\cdot + \beta^4 m^4 \pi^4 \left(\cot^4\alpha + \frac{\zeta}{\sin^4\alpha} \right)\}$,

$$p_{ijm} = \int_0^1 \cos i\pi X \cos j\pi X \sin m\pi X \, dX =$$

$$\frac{1}{2\pi} \left(\frac{1}{m+i+j} + \frac{1}{m-i-j} + \frac{1}{m+i-j} + \frac{1}{m-i+j} \right),$$

$$q_{ijm} = \int_0^1 \sin i\pi X \sin j\pi X \sin m\pi X \, dX =$$

$$\frac{1}{2\pi}\left(\frac{-1}{m+i+j} - \frac{1}{m-i-j} + \frac{1}{m+i-j} + \frac{1}{m-i+j}\right).$$

And the equations of various boundary conditions can be expressed using f_m, g_m for example, in the case of simply supported, symmetrical part; from Eqs. (4b) and Eqs. (5)

$$f_{ms} = f_{ms}'' = g_{ms} = g_{ms}'' = 0, \text{ on } Y = \frac{1}{2} \tag{7a}$$

antisymmetrical part;

$$f_{ma} = f_{ma}'' = g_{ma} = g_{ma}'' = 0, \text{ on } Y = \frac{1}{2} \tag{7b}$$

2) Presentation of the Solution

Equations (6) may be treated like linear equations by regarding the partially nonlinear terms: Φ_{ms}, Ψ_{ms}, Φ_{ma} and Ψ_{ma} as the functions of Y. So, the solution of Eqs. (6) can be obtained by superposition of a particular integral and the solution of the corresponding homogeneous equation.

a) Homogeneous solution

The forms of homogeneous solution: g_{msh}, f_{msh}, g_{mah}, f_{mah} vary according to reticular parameters: α, γ, ζ; for example, the following solutions are obtained when γ, $\zeta < 8\cos^4\alpha$:

$$\left.\begin{aligned} g_{msh} &= C_{1ms}\sin\lambda_{2m}Y \operatorname{sh}\lambda_{1m}Y + C_{2ms}\cos\lambda_{2m}Y \operatorname{ch}\lambda_{1m}Y \\ g_{mah} &= C_{1ma}\cos\lambda_{2m}Y \operatorname{sh}\lambda_{1m}Y + C_{2ma}\sin\lambda_{2m}Y \operatorname{ch}\lambda_{1m}Y \\ f_{msh} &= \sum_P D_{pms}\operatorname{ch}\xi_{pm}Y, \qquad f_{mah} = \sum_P D_{pma}\operatorname{sh}\xi_{pm}Y \end{aligned}\right\} \tag{8}$$

where $p = 1,2$ C_{pms}, C_{pma}, D_{pms}, D_{pma} are integration constants, $\operatorname{sh} \equiv \sinh$, $\operatorname{ch} \equiv \cosh$, $\lambda_{2m}^{1m} = \dfrac{\beta m\pi}{2\sin\alpha}\sqrt{2\sqrt{\cos^4\alpha+\gamma} \pm \left(2\cos^2\alpha - \dfrac{\gamma}{\cos^2\alpha}\right)}$, $\xi_{2m}^{1m} = \dfrac{\beta m\pi}{\sin\alpha}\sqrt{3\cos^2\alpha \pm \sqrt{8\cos^4\alpha - \zeta}}$

b) Particular solution

Particular solutions: g_{msp}, f_{msp}, g_{map}, f_{map} are expressed by the form in Fourier trigonometric series over the interval $(-0.5, 0.5)$

$$\left.\begin{aligned} g_{msp} &= \sum_{k_s} S_{k_s m}\cos k_s\pi Y, \qquad f_{msp} = \sum_{k_s} t_{k_s m}\cos k_s\pi Y \\ g_{map} &= \sum_{k_a} S_{k_a m}\sin k_a\pi Y, \qquad f_{map} = \sum_{k_a} t_{k_a m}\sin k_a\pi Y \end{aligned}\right\} \tag{9}$$

where $k_s = 0, 2, 4, 6\cdots$, $k_a = 2, 4, 6\cdots$, $S_{k_s m}$, $t_{k_s m}$, $S_{k_a m}$, $t_{k_a m}$ are Fourier coefficients. Similarly, the expansions of Φ_{ms}, Ψ_{ms}, Φ_{ma} and Ψ_{ma} into Fourier trigonometric series for $|Y| \leqq 0.5$ become

$$\left.\begin{aligned} \Phi_{ms} &= \sum_{k_s} \rho_{k_s m} \cos k_s \pi Y, & \Psi_{ms} &= \sum_{k_s} \varepsilon_{k_s m} \cos k_s \pi Y \\ \Phi_{ma} &= \sum_{k_a} \rho_{k_a m} \sin k_a \pi Y, & \Psi_{ma} &= \sum_{k_a} \varepsilon_{k_a m} \sin k_a \pi Y \end{aligned}\right\} \tag{10}$$

where coefficients: $\rho_{k_s m}$, $\varepsilon_{k_s m}$, $\rho_{k_a m}$, $\varepsilon_{k_a m}$ can be determined by the following equations:

$$(\rho_{k_s m}, \varepsilon_{k_s m}) = \begin{cases} 4\int_0^{1/2} (\Phi_{ms}, \Psi_{ms}) \cos k_s \pi Y \, dY; & k_s \geqq 2 \\ 2\int_0^{1/2} (\Phi_{ms}, \Psi_{ms}) \, dY & ; k_s = 0 \end{cases}$$

$$(\rho_{k_a m}, \varepsilon_{k_a m}) = 4\int_0^{1/2} (\Phi_{ma}, \Psi_{ma}) \sin k_a \pi Y \, dY \tag{11}$$

It is pointed out that the values of integration in Eq. (11) are expressed explicitly without performing a numerical integration. Substituting Eqs. (9), (10) into Eqs. (6) and comparing the coefficients, Eqs. (12) are obtained:

$$\left.\begin{aligned} &\pi^4\left\{k_s^4 + k_s^2 m^2 \beta^2 \left(\frac{\gamma}{\sin^2\alpha\cos^2\alpha} - 2\cot^2\alpha\right) + m^4\beta^4\left(\cot^4\alpha + \frac{\gamma}{\sin^4\alpha}\right)\right\} S_{k_s m} = \rho_{k_s m} \\ &\frac{3}{32}\pi^4\left\{k_s^4 + k_s^2 m^2 \beta^2\, 6\cot^2\alpha + m^4\beta^4\left(\cot^4\alpha + \frac{\zeta}{\sin^4\alpha}\right)\right\} t_{k_s m} = \varepsilon_{k_s m} \\ &\pi^4\left\{k_a^4 + k_a^2 m^2 \beta^2 \left(\frac{\gamma}{\sin^2\alpha\cos^2\alpha} - 2\cot^2\alpha\right) + m^4\beta^4\left(\cot^4\alpha + \frac{\gamma}{\sin^4\alpha}\right)\right\} S_{k_a m} = \rho_{k_a m} \\ &\frac{3}{32}\pi^4\left\{k_a^4 + k_a^2 m^2 \beta^2\, 6\cot^2\alpha + m^4\beta^4\left(\cot^4\alpha + \frac{\zeta}{\sin^4\alpha}\right)\right\} t_{k_a m} = \varepsilon_{k_a m} \end{aligned}\right\} \tag{12}$$

3) Numerical Method

Solving Eqs. (1) subjected to Eqs. (3) and (4) results in finding a solution to Eqs. (7), (12) concerning coefficients: D_{pms}, D_{pma}, C_{pms}, C_{pma}, $t_{k_s m} \cdot t_{k_a m}$, $S_{k_s m}$, $S_{k_a m}$, ($p = 1, 2$, $m = 1, 3, 5\cdots$, $k_s = 0, 2, 4, 6\cdots$, $k_a = 2, 4, 6, \cdots$), Λ_s, Λ_a. A solution to these nonlinear simultaneous algebraic equations can be obtained by applying the Newton-Raphson procedure.

4) Analytical Method for the Case of Isotropic Reticular Pattern

When the reticular pattern is isotropic ($\gamma = \zeta = 0.5$, $\alpha = 60°$.), Eqs. (1) are identical with Donnell's Equations setting Poisson's ratio 1/3. Therefore, the general buckling problems of isotropic C. R. S. R. are mechanically equivalent to that of isotropic monocoque cylindrical shells. In the case of isotropics, characteristic equations of Eqs. (6) have equal roots, so the forms of the homogeneous solutions should be different from the function represented in Eqs. (8), as previously mentioned. However, using the forms of Eqs. (8), the isotropic problem can also be analyzed as follows.

Introducing small constant: η, Eqs. (6) are transformed into Eqs. (13):

$$\left.\begin{aligned} &\square_{1m}(g_{ms}, g_{ma}) = (\Phi_{ms}, \Phi_{ma}) + 2\beta^2 m^2 \pi^2 \eta \, (g_{ms}'', g_{ma}'') \\ &\frac{3}{32}\square_{2m}(f_{ms}, f_{ma}) = (\Psi_{ms}, \Psi_{ma}) - \frac{3}{32}\beta^2 m^2 \pi^2 \cdot 2\eta \, (f_{ms}'', f_{ma}'') \end{aligned}\right\} \tag{13}$$

where $\square_{2m}^{1m} = \cdots\cdots - 2\beta^2 m^2\pi^2(1 \mp \eta)\cdot\cdot + \beta^4 m^4\pi^4$, so when $\eta > 0$ we can use the form of Eqs. (8) setting $\lambda_{1m} = \frac{\sqrt{2}}{2}\beta m\pi\sqrt{2-\eta}$, $\lambda_{2m} = \frac{\sqrt{2}}{2}\beta m\pi\sqrt{\eta}$, $\xi_{2m}^{1m} = \beta m\pi\sqrt{1+\eta \pm \sqrt{2\eta+\eta^2}}$.

IV. NUMERICAL RESULTS AND DISCUSSION

Based upon the analytical method represented in the previous section, in isotropic ($\gamma = \zeta = 0.5$, $\alpha = 60°$.), the general buckling behaviors of C.R.S.R. subjected to a uniformly normal load are investigated in the range of $\beta = 0.5 \sim 1.$, $\mu_h = 100 \sim 300$ with pinned, simply supported or free generator edges. Furthermore, when generator edges are simply supported, the effects of the imperfection on the general buckling behavior are investigated by applying the unsymmetrical load as shown in Fig. 1c. The number of terms in series and η will influence the accuracy of the nonlinear solution. After verifying the convergency of a few numerical examples[5] in this numerical computations, m, k_s, k_a are adopted up to 2, 4, 4 terms respectively for the case of pinned or simply supported, and 3, 5, 5 terms for free edges, besides $\eta = 0.005$.

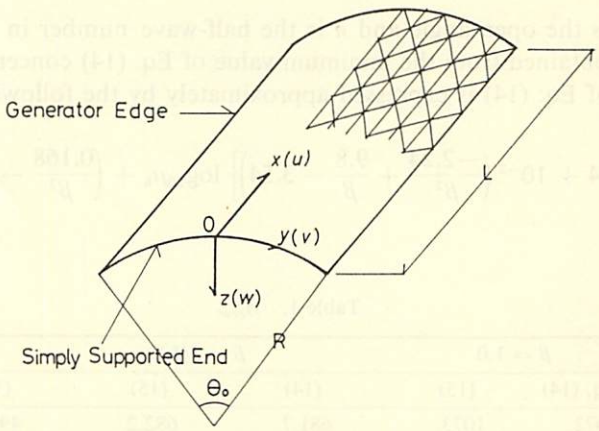

Fig. 1a. Geometry.

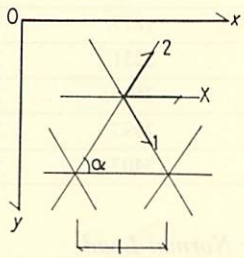

Fig. 1b. Reticular pattern.

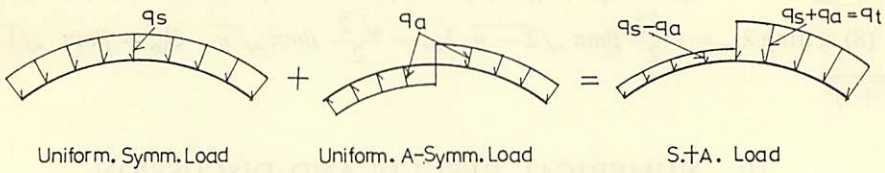

Fig. 1c. Load distribution for circumferential direction.

1) Classical Buckling Load

The buckling loads obtained from nonlinear analysis are expressed by the ratio of the classical buckling load Λ_{cro} for the closed cylinder subjected to a uniformly normal load. When the two ends are simply supported, from Eqs. (1) setting $\gamma = \zeta = 0.5, \alpha = 60°$, Λ_{cro} is given by the following equation:

$$\Lambda_{cro} = \frac{q_{cro}}{E_h}\left(\frac{B}{t_h}\right)^4 = \mu_h{}^3\left[\frac{1}{(\theta_0 n)^2\left\{\left(\frac{\theta_0 n}{\beta\pi}\right)^2+1\right\}^2} + \frac{3}{32}\frac{1}{\mu_h{}^2}(\theta_0 n)^2\left\{1+\left(\frac{\beta\pi}{\theta_0 n}\right)^2\right\}\right]\Bigg|_{\min.} \tag{14}$$

where θ_0 indicates the open angle and n is the half-wave number in the circumferential direction. Λ_{cro} is obtained from the minimum value of Eq. (14) concerning $\theta_0 n$. As shown in Table 1; Λ_{cro} of Eq. (14) is expressed approximately by the following equation:

$$\log_{10}\Lambda_{cro} = \left\{1.4 + 10^{-2}\left(\frac{-2.24}{\beta^2}+\frac{9.8}{\beta}-3.54\right)\right\}\log_{10}\mu_h + \left(\frac{0.168}{\beta^2}-\frac{0.897}{\beta}+0.879\right). \tag{15}$$

Table 1. Λ_{cro}.

	$\beta = 1.0$		$\beta = 1/1.5$		$\beta = 0.5$	
μ_h	Eq. (14)	(15)	(14)	(15)	(14)	(15)
100	1072.	1073.	681.7	682.2	499.6	500.0
125	1476.	1479.	943.5	945.2	693.2	694.3
150	1919.	1923.	1231.	1234.	906.3	907.9
175	2397.	2401.	1543.	1545.	1137.	1139.
200	2909.	2910.	1877.	1878.	1385.	1386.
225	3451.	3448.	2231.	2231.	1648.	1648.
250	4023.	4013.	2605.	2602.	1926.	1925.
275	4622.	4604.	2997.	2991.	2217.	2214.
300	5248.	5219.	3407.	3397.	2522.	2517.

2) Results under a Uniformly Normal Load

Two types of general buckling phenomena in the C.R.S.R. subjected to a uniformly normal load are studied numerically here. One is snap-through buckling with the deflection pattern symmetrical with respect to both the center lines, and the other is bifurcation buck-

ling with the buckling mode symmetrical with respect to the central arc and antisymmetrical with reference to the central generator. The numerical results are shown in Figs. 2–4 in each boundary condition.

(a) Pinned edge: $\frac{\Lambda_{cr}}{\Lambda_{cro}}$ is larger than unity, as shown in Fig. 2a, where Λ_{cr} is the critical load of a uniformly normal load. Snap-through buckling occurs for the case of ($\beta = 1$, $100 \leqq \mu_h \leqq 150$), $\left(\beta = \frac{1}{1.5}, \ 100 \leqq \mu_h \leqq 275\right)$, ($\beta = 0.5$, $100 \leqq \mu_h \leqq 300$) and half-wave number of its buckling mode N is 3. For $\beta = 1$, $175 \leqq \mu_h \leqq 275$, as shown in Fig. 2b,c, bifurcation buckling occurs before the local maximum load is attained, and $N = 4$. In each range, $\frac{\Lambda_{cr}}{\Lambda_{cro}}$ is approximately expressed by using constants, k_1, k_2, k_3 as in the following equation.

$$\frac{\Lambda_{cr}}{\Lambda_{cro}} = \sum_{i=1}^{3} k_i \mu_h^{\,i-2} \tag{16}$$

For $\beta = 1$, $\mu_h = 300$, just after bifurcation buckling, an incremental deflection of $N = 5$ yields newly as shown in Fig.2c, therefore both types of buckling may occur adjacent to each other.

(b) Simply supported edge: $\frac{\Lambda_{cr}}{\Lambda_{cro}}$ is less than unity, as shown in Fig.3a. For $\mu_h \geqq 150$, it can be pointed out that the smaller β, the higher becomes $\frac{\Lambda_{cr}}{\Lambda_{cro}}$. For $\beta = 1$, $\mu_h \geqq 225$, snap-through buckling occurs without bifurcation buckling, and $N = 3$. For the other parameters, bifurcation buckling precedes and $N = 2$. For ($\beta = 1$, $100 \leqq \mu_h \leqq 200$), ($\beta = \frac{1}{1.5}$, $150 \leqq \mu_h \leqq 300$), $\frac{\Lambda_{crB}}{\Lambda_{cro}}$ are approximately expressed by the following equation.

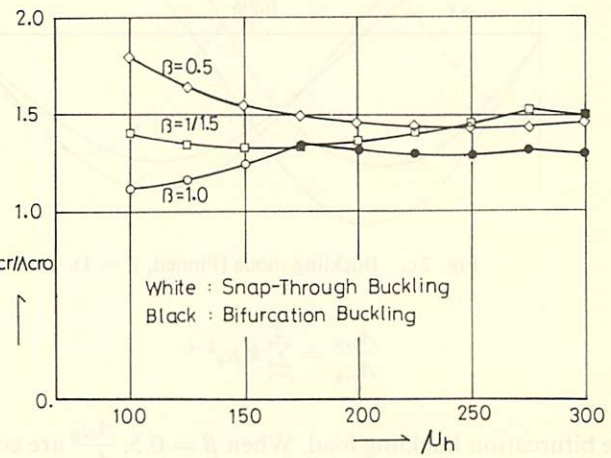

Fig. 2a. $\Lambda_{cr}/\Lambda_{cro}$ (Pinned).

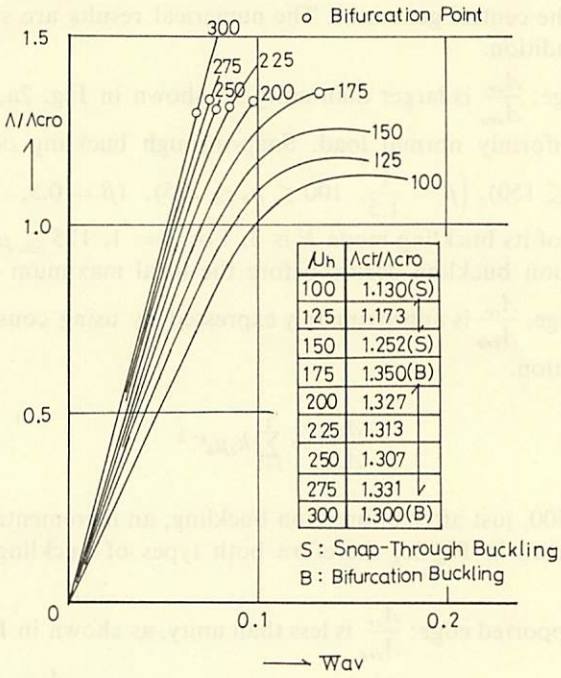

Fig. 2b. Λ/Λ_{cro}-W_{av} (Pinned, $\beta = 1$).

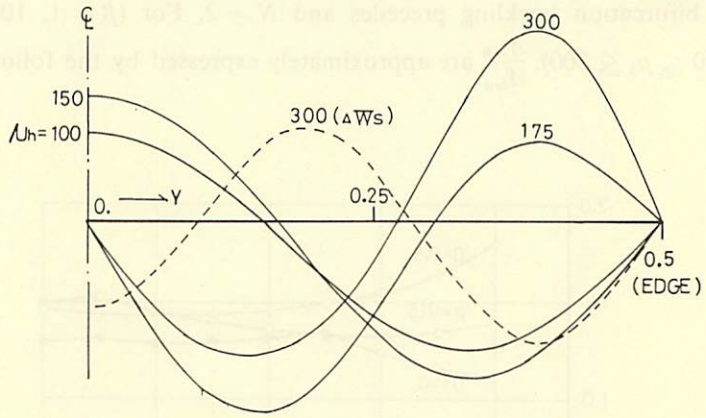

Fig. 2c. Buckling mode (Pinned, $\beta = 1$).

$$\frac{\Lambda_{crB}}{\Lambda_{cro}} = \sum_{i=1}^{2} k_i \mu_n^{2-i} \tag{17}$$

where Λ_{crB} is the bifurcation buckling load. When $\beta = 0.5$, $\frac{\Lambda_{crB}}{\Lambda_{cro}}$ are considered to be nearly

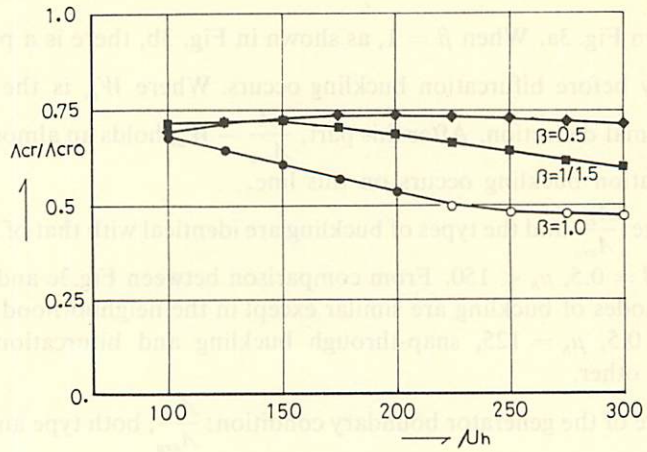

Fig. 3a. $\Lambda_{cr}/\Lambda_{cro}$ (Simply supported = s.s.).

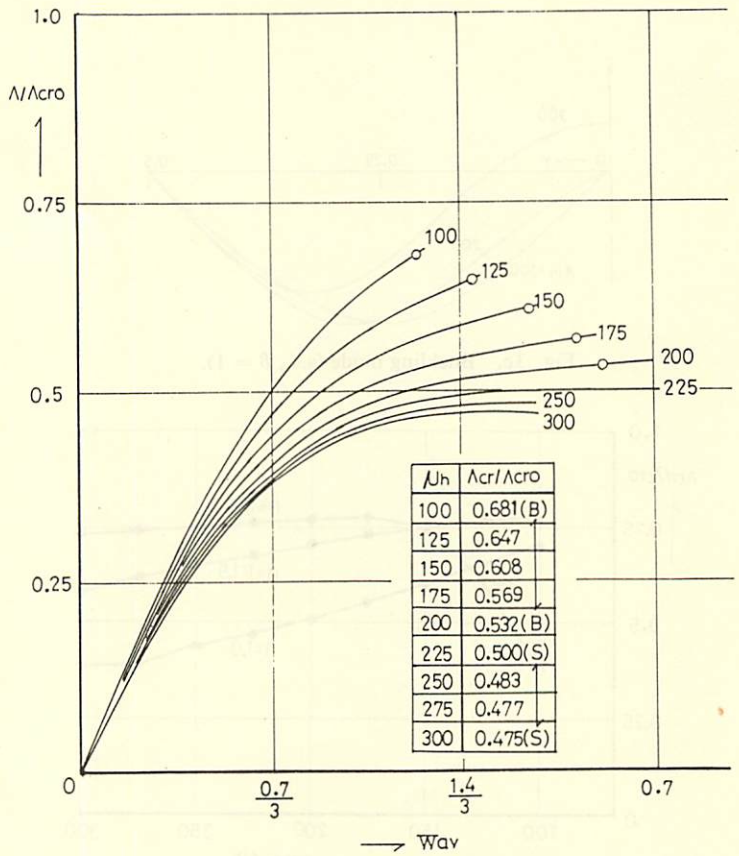

Fig. 3b. Λ/Λ_{cro}-W_{av} (s.s., $\beta = 1$).

constant as shown Fig. 3a. When $\beta = 1$, as shown in Fig. 3b, there is a part where $\frac{d\left(\frac{\Lambda}{\Lambda_{cro}}\right)}{d(W_{av})}$ decreases greatly before bifurcation buckling occurs. Where W_{av} is the average of non-dimensional normal deflection. After this part, $\frac{\Lambda}{\Lambda_{cro}} - W_{av}$ holds an almost linear relation, and then bifurcation buckling occurs on this line.

(c) Free edge: $\frac{\Lambda_{cr}}{\Lambda_{cro}}$ and the types of buckling are identical with that of simply supported edge excluding $\beta = 0.5$, $\mu_h < 150$. From comparison between Fig.3c and Fig.4c, it can be said that both modes of buckling are similar except in the neighborhood of the generator edges. For $\beta = 0.5$, $\mu_h = 125$, snap-through buckling and bifurcation buckling occur adjacent to each other.

(d) Influence of the generator boundary condition: $\frac{\Lambda_{cr}}{\Lambda_{cro}}$, both type and mode of buck-

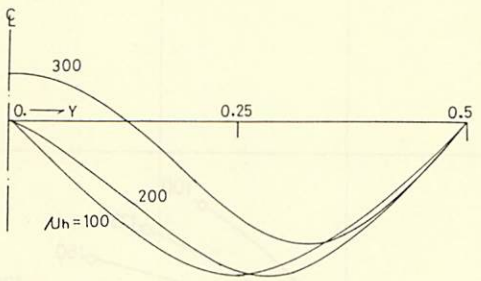

Fig. 3c. Buckling mode (s.s., $\beta = 1$).

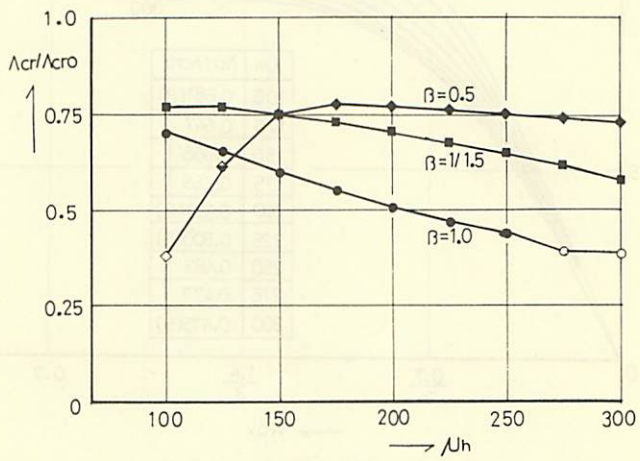

Fig. 4a. $\Lambda_{cr}/\Lambda_{cro}$(Free).

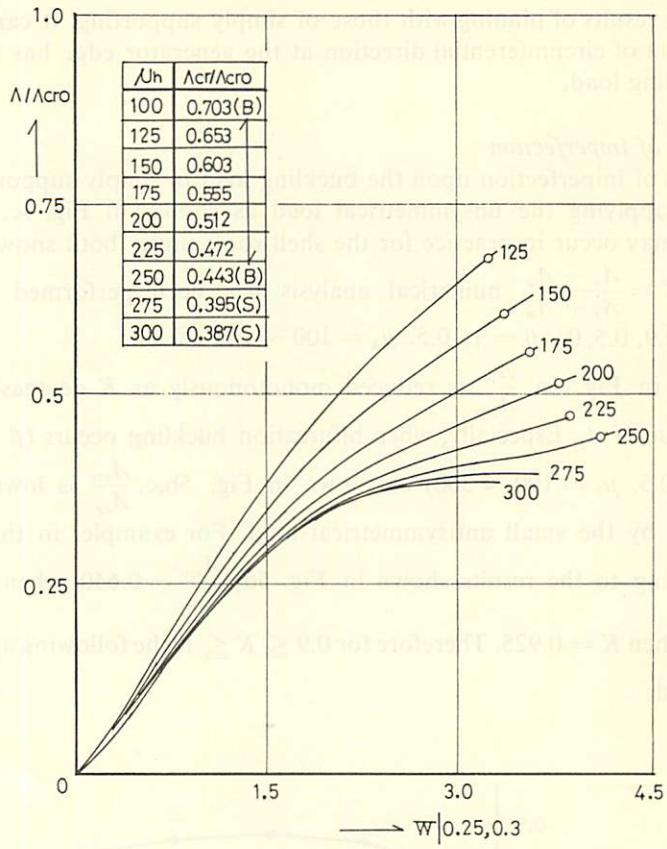

Fig. 4 b. Λ/Λ_{cro}-$W|0.25, 0.3$ (Free, $\beta = 1$).

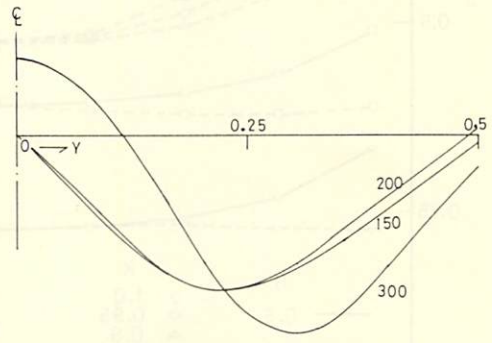

Fig. 4c. Buckling mode (Free, $\beta = 1$).

ling in case of a simply supported edge are identical with that for free edge excluding $\beta = 0.5$, $\mu_h < 150$, in spite of the different deflection and stress at the onset of buckling.

Comparing the results of pinning with those of simply supporting, it can be pointed out that the restraint of circumferential direction at the generator edge has a great influence upon the buckling load.

3) Effects of Imperfection

The effects of imperfection upon the buckling load in simply supported edges are investigated by applying the unsymmetrical load as shown in Fig. 1c. Such an unsymmetrical load may occur in practice for the shell roofs under both snow and wind loads. Introducing $K = \frac{\Lambda_s - \Lambda_a}{\Lambda_s + \Lambda_a}$, numerical analysis has been performed in the range of $K = 1., 0.95, 0.9, 0.5, 0., \beta = 1, 0.5. \mu_h = 100 \sim 300$ @ 50.

As shown in Fig. 5a, $\frac{\Lambda_{scr}}{\Lambda_{cro}}$ is reduced monotonously as K decreases, where Λ_{scr} is the critical value of Λ_s. Especially, when bifurcation buckling occurs ($\beta = 1, \mu_h = 100 \sim 200$ and $\beta = 0.5, \mu_h = 100 \sim 300$) as shown in Fig. 5b,c, $\frac{\Lambda_{scr}}{\Lambda_{cr}}$ is lowered by a considerable amount by the small antisymmetrical load. For example, in the case of $\beta = 1$, $\mu_h = 100$, adding to the results shown in Fig. 5d, $\frac{\Lambda_{scr}}{\Lambda_{cro}} = 0.640$ when $K = 0.975$, and $\frac{\Lambda_{scr}}{\Lambda_{cro}} = 0.597$ when $K = 0.925$. Therefore for $0.9 \leqq K \leqq 1$, the following approximate equation is obtained:

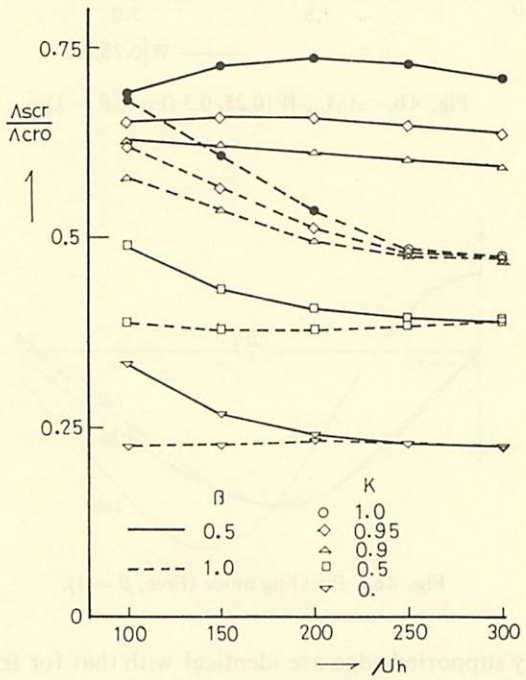

Fig. 5a. $\Lambda_{scr}/\Lambda_{cro}$.

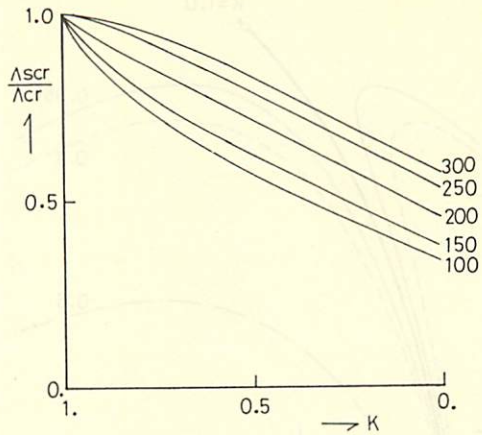

Fig. 5b. $\Lambda_{scr}/\Lambda_{cr}$-$k$ ($\beta = 1$).

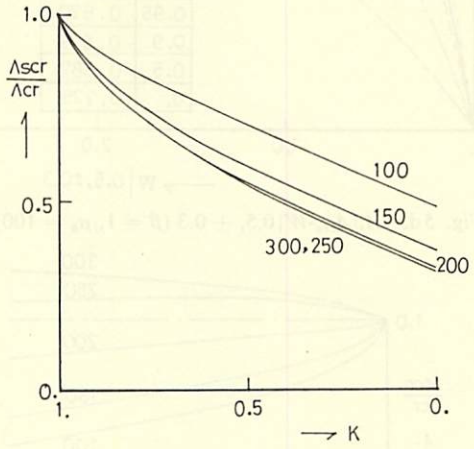

Fig. 5c. $\Lambda_{scr}/\Lambda_{cr}$-$k$ ($\beta = 0.5$).

$$\frac{\Lambda_{scr}}{\Lambda_{cr}} - 1 = -1.053\left(\frac{1-k}{1+k}\right)^{\frac{2}{3}} \tag{18}$$

Eq. (18) indicates a two-thirds power law for the unstable symmetric point of bifurcation.[6]

For $\beta = 1$ and $K = 0.5$, 0, $\frac{\Lambda_{scr}}{\Lambda_{cro}}$ is almost constant at 0.380 and 0.225, respectively, throughout the whole range of μ_n considered here. Therefore, it is considered that $\frac{\Lambda_{scr}}{\Lambda_{cro}}$ is the function of K only in the range of relatively small K.

When bifurcation buckling occurs, $\frac{\Lambda_{tcr}}{\Lambda_{cr}}$ is less than unity, as shown in Fig. 5e,f. Where Λ_{tcr} is the critical value of Λ_t ($=\Lambda_s + \Lambda_a$). For the same K, it can be pointed out

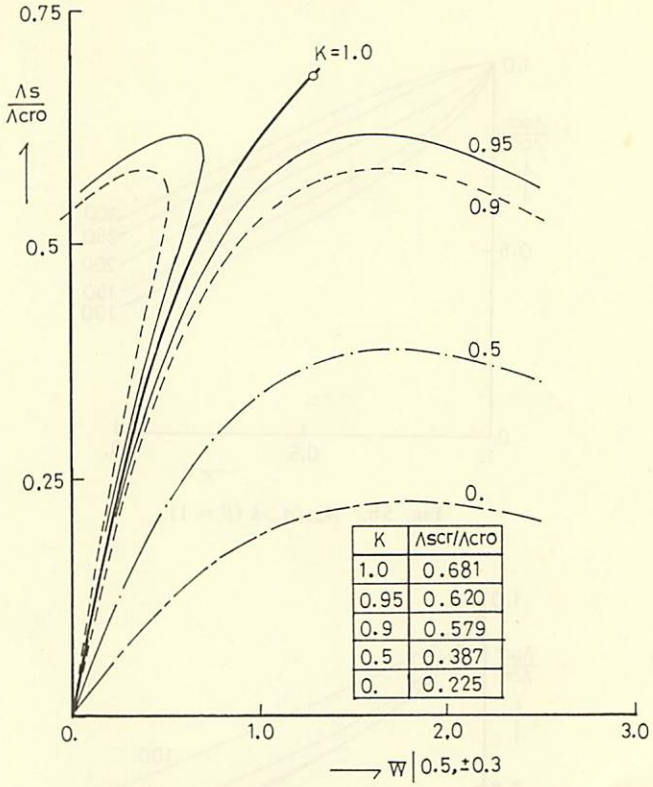

Fig. 5d. Λ_s/Λ_{cro}-$W|0.5, \pm 0.3$ ($\beta = 1, /\mu_h = 100$).

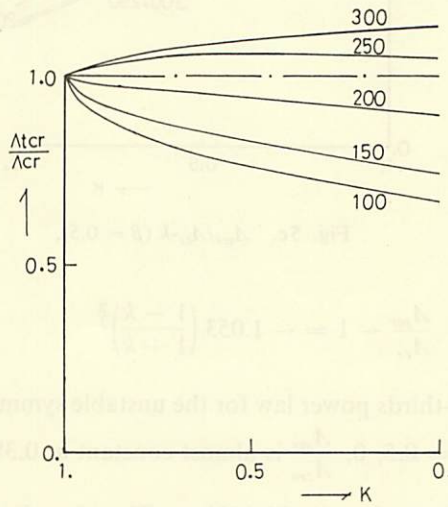

Fig. 5e. $\Lambda_{tcr}/\Lambda_{cr}$-$K$ ($\beta = 1$).

that the smaller μ_h with $\beta = 1$ and the larger μ_h with $\beta = 0.5$, the smaller $\frac{\Lambda_{tcr}}{\Lambda_{cr}}$ becomes. On the other hand, when snap-through buckling occurs ($\beta = 1$, $\mu_h = 225 \sim 300$),

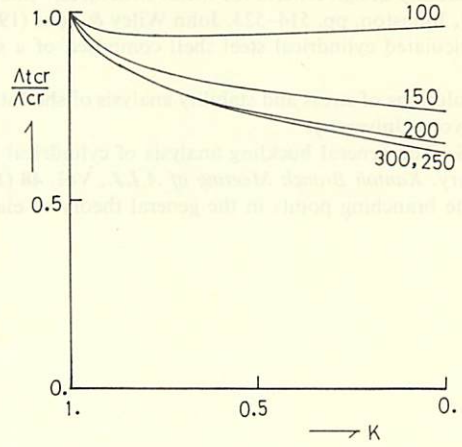

Fig. 5 f. $\Lambda_{tcr}/\Lambda_{cr}$-$k(\beta = 0.5)$.

$\frac{\Lambda_{tcr}}{\Lambda_{cr}}$ is larger than unity. For the same K, it can be pointed out that the larger μ_h, the larger $\frac{\Lambda_{tcr}}{\Lambda_{cr}}$ becomes.

Consequently, for $\beta = 1$, around $\mu_h = 225$, in which both snap-through and bifurcation buckling load are almost same, $\frac{\Lambda_{tcr}}{\Lambda_{cr}}$ is nearly unity without regard to K.

V. CONCLUSION

An approximate analytical method of the nonlinear basic equations which govern the general buckling phenomena of C.R.S.R. subjected to a normal load has been developed under the boundary conditions that the two ends of the structure are simply supported and the two generator edges are arbitrary.

Based upon this method, the general buckling behaviors of isotropic C.R.S.R. have been investigated numerically under shell geometries in the range of $0.5 \leqq \beta \leqq 1{,}100 \leqq \mu_h \leqq 300$, pinned., simply supported and free generator boundaries, unsymmetrical loading parameter $0. \leqq K \leqq 1$, in compared with classical buckling load of the closed cylinder subjected to a uniformly normal load.

Acknowledgment

The author deeply wishes to thank Dr. Sadaichi Terada and Dr. Fumihito Itoh Professors of Tokyo Metropolitan University, for their valuable discussions and suggestions in this study.

REFERENCES

1) Douglas, T. W., Membrane forces and buckling in reticulated shells. *Proc. of ASCE, ST1*, February, (1965).

2) Buchert, K. P., Guide to stability design criteria for metal structures. "Shell and Shell-Like Structures" 3rd. Ed. *Edited by* Bruce G. Johnston. pp. 514–523. John Wiley & Sons (1976).
3) Chiba, N. and others, Reticulated cylindrical steel shell composed of a single layer with wide flange shapes. *Pro. IASS* (1971).
4) Matsui, T., Methods and solutions of stress and stability analysis of shell structures, chapter 6, February (1977). Doctoral Thesis, Kyoto Universrty.
5) Kokawa, T. and Terada, S., The general buckling analysis of cylindrical reticulated shell roofs under arbitrary generator boundary. *Kantoh Branch Meeting of A.I.J.*, Vol. **48** (1978).
6) Thompson, J.M.T., Discrete branching points in the general theory of elastic stability. *J. Mech. Phys. Solids*. Vol. **13**, (1965).